Capillary flow as the cause of ring stains from dried liquid drops

Robert D. Deegan, Olgica Bakajin, Todd F. Dupont, Greg Huber, Sidney R. Nagel, Thomas A. Witten
James Franck Institute, 5640 South Ellis Ave, Chicago, IL 60637, USA
typeset July 15, 1997

When a spilled drop of coffee dries on a solid surface, it leaves a dense, ring-like stain along the perimeter (Figure 1a). The coffee—initially dispersed over the entire drop—becomes concentrated into a tiny fraction of it. Such ring deposits are commonplace wherever drops containing dispersed solids evaporate on a surface. Thus ring deposits influence printing, washing and coating processes [1–5]. They provide a potential means to write or deposit a fine pattern onto a surface. Here we ascribe the deposition to a previously unexplored form of capillary flow: the contact line of the drying drop is pinned so that liquid evaporating from the edge must be replenished by liquid from the interior (Figure 2). The resulting outward flow can carry virtually all the dispersed material to the edge. This mechanism predicts a distinctive power-law growth of the ring mass with time—a law independent of the particular substrate, carrier fluid or deposited solids. We have verified this law by microscopic observations of colloidal fluids.

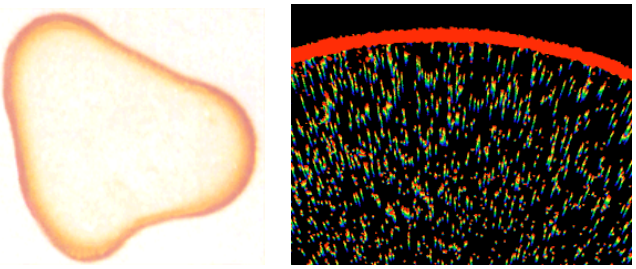

FIG. 1. a) A 2-cm-diameter drop of coffee containing one-weight-percent solids has dried to form a perimeter ring, accentuated in regions of high curvature. b) Video micrographs showing dispersion of fluorescent one-micron polystyrene spheres in water during evaporation, as described in the text. Multiple exposure shows different times in different colors to indicate the motion. Earliest time (blue) is 3 sec before latest time (red).

Our qualitative observations show that rings form for a wide variety of substrates, dispersed materials (solutes), and carrier liquids (solvents), as long as (1) the solvent meets the surface at a nonzero contact angle, (2) the contact line is pinned to its initial position, and (3) the solvent evaporates. In addition, we found that mechanisms typically responsible for solute transport—surface tension gradients, solute diffusion, electrostatic, and gravity effects—are negligible in ring formation. Based on these findings, we have identified the minimal ingredients for a quantitative theory. The phenomenon is due to a geometrical constraint: the free surface, constrained by a pinned contact line, squeezes the fluid outward to compensate for evaporative losses. We first describe the main features and results of our theory and then show our experimental tests of its validity.

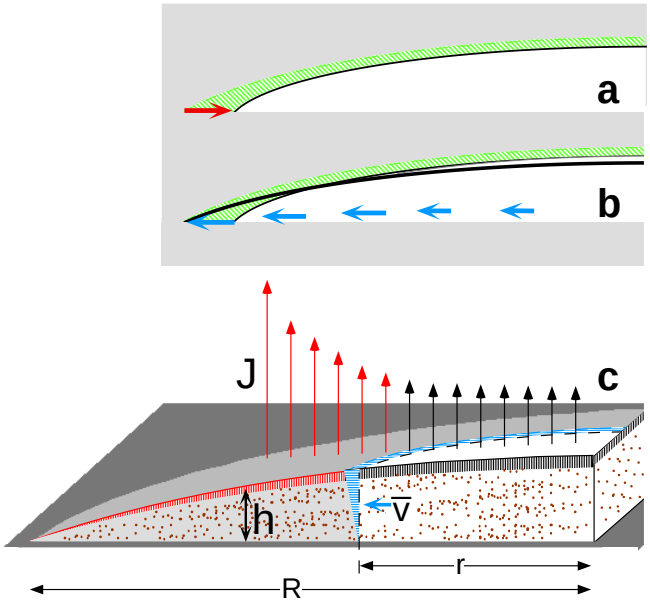

FIG. 2. Mechanism of outward flow during evaporation. Pictures **a** and **b** show an increment of evaporation viewed in cross section. Picture **a** shows the result of evaporation without flow: the droplet shrinks. Picture **b** shows the compensating flow needed to keep the contact line fixed. Picture **c** defines quantities responsible for flow. Vapor leaves at a rate per unit area $J(r)$. The removed liquid contracts the height $h(r)$ vertically, vacating the vertically striped region in a short time Δt. The volume of this striped region is equal to the volume removed by J. But in the shaded annular region the red-striped volume is *smaller* than the volume removed by J there (red arrows). Thus liquid flows outward to supply the deficit volume: fluid at r sweeps out the blue-striped region in time Δt. Its volume is the deficit volume; its depth-averged speed is $\bar{v}(r)$.

Figure 2 sketches the factors leading to outward flow in a small, thin, dilute, circular drop of fixed radius R slowly drying on a solid surface. The evaporative flux $J(r)$ reduces the height $h(r)$ at every point r. If there were no flow, the evaporation would alter the height pro-

file as sketched in Figure 2a. At the perimeter, all the liquid would be removed and the drop would shrink. But the radius of the drop cannot shrink, since its contact line is pinned. To prevent the shrinkage, liquid must flow outward as in Figure 2b. The complete flow profile $\bar{v}(r)$ can be found as sketched in Figure 2c. The height profile must maintain the spherical cap shape dictated by surface tension. Thus during a short time Δt the vertically striped region must be removed from each point r of the surface. This is different from the amount removed from that point owing to evaporation, shown in color in Figure 2a. Radial flow must make up for this difference. If the evaporative flux $J(r)$ is known, the flow velocity $\bar{v}(r)$ is thereby determined.

The evaporative flux has a universal form that depends only on the shape of the drop (for example see: [6,**?**]). In the evaporation process liquid molecules interchange rapidly between the surface and the adjacent air, so that this air is saturated with vapor. Since the air at infinity is not saturated, the vapor diffuses outward. At the surface of the drop (which is the only region where we need to calculate the evaporation current) the vapor quickly establishes a steady-state concentration profile $\phi(\vec{r})$ which obeys the steady-state diffusion equation $\nabla^2\phi = 0$. At infinity, ϕ is the ambient concentration ϕ_∞. At the drop surface ϕ is fixed at the saturation concentration ϕ_s. The derivitive at the surface gives the desired evaporating flux $J(r) = -D\nabla\phi$, where D is the diffusivity of the vapor in air.

We may find the flux J by solving an equivalent electrostatic problem [8], wherein ϕ is an electrostatic potential and the drop, with its fixed potential, is a conductor. (On the substrate surface beyond the drop there is no flux, so that the normal derivitive of ϕ is zero there. That surface is in effect a reflection plane of symmetry and the opening angle of the conducting wedge is twice the contact angle that the drop makes with the substrate.) The sharp wedge-shaped boundary of the drop and its reflection leads to a diverging normal derivitive (electric field or evaporative flux) as r approaches the contact line. For a drop with contact angle θ_c, this divergence has the form [9]: $J(r) \sim (R-r)^{-\lambda}$, where $\lambda = \frac{\pi-2\theta_c}{2\pi-2\theta_c}$. As the contact angle decreases towards zero, λ increases towards 1/2.

The initial deposition over times much shorter than the drying time depends sensitively on this diverging flux. To replace the diverging flux requires a diverging velocity near the perimeter: $\bar{v} \sim J \sim (R-r)^{-\lambda}$. We now consider the mass of solute, $M(r,t)$ beyond distance r from the center at time t. Near the contact line the *initial* mass $M(r,0)$ is proportional to the volume of this wedge shaped region: $M(r,0) \sim (R-r)^2$. All this mass will be entrained in the ring in the time t required for a point starting at r_t to move to the contact line:

$$t = \int_{r_t}^{R} dr/\bar{v} \sim (R-r_t)^{1+\lambda}, \qquad (1)$$

since $\bar{v}(r) \sim (R-r)^{-\lambda}$. Substituting for r_t in terms of t into $M(r_t,0)$ yields a power law for the early time growth of the ring: $M(R,t) = M(r_t,0) \sim t^{2/(1+\lambda)}$.

At late times, the theory predicts *complete* transfer of the solute to the perimeter. As the time t approaches the drying time t_f, the height $h(r)$ decreases to zero as $(t_f - t)$. But the outward current $h(r)\bar{v}(r)$ must stay constant with time in order to replenish the constant evaporation flux J. Thus $\bar{v}$ must grow as $(t_f - t)^{-1}$. This diverging velocity leads to a diverging displacement of any point $r > 0$. Thus all initial points $r > 0$ are carried to the perimeter before the drying time t_f.

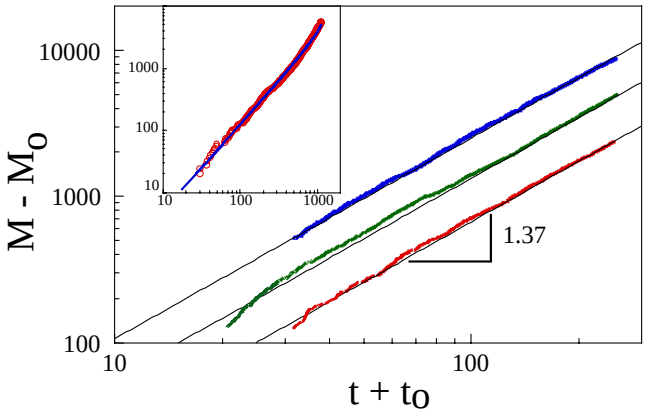

FIG 3. Double-logarithmic plot of ring mass $M(R,t)$ versus time t for times from 10 to 250 seconds after placement of the drop on the surface, for three different drops whose total drying time was about 800 sec. $M(R,t)$ is measured in number of particles. Particle number is counted in a sector of the ring similar to that shown in Figure 1b. An offset $M_0 = 2$ was subtracted from the lowest curve to account for early non-steady-state deposition. $M_0 = 50$ and 40 for the middle and upper curves. The upper curve coincided with the middle one and was shifted up by a factor of 2 for clarity. An offset $t_0 = 11$ sec, 13 sec and 10 sec was added to the time axis. The solid lines show the power law $(M-M_0) = \text{const}\ (t+t_0)^{1.37}$. Inset shows $M(R,t)$ versus t for the entire 1300-sec drying time. Circles: data obtained from ten-micron spheres via counting. Roughly 90 percent of the particles were observed to go to the contact line. Solid line: theoretical prediction determined numerically.

To test these predictions we used drops of distilled water which contained charge-stabilized surfactant-free polystyrene microspheres [Interfacial Dynamics, Portland, Oregon] at a starting volume fraction of 10^{-4}. The spheres were so dilute that they could be regarded as an ideal solution except in the very narrow ring region. Droplets with nominal radius 4 mm were deposited on glass microscope slides and allowed to dry in a large enclosure with measured ambient temperature and humid-

ity. The volume of the droplet was inferred by weighing the slide during drying. The volume decreased at a rate which agreed within two percent with that expected for steady-state vapor-diffusion-limited evaporation, using tabulated values [10] for the water diffusivity in air and for the saturated vapor concentration.

In a separate experiment we observed the solute ring deposition by viewing the migration of one-micron microspheres in a video microscope during drying, as shown in Figure 1b. By automatically analyzing [11] the video record, the depth-averaged velocity $\bar{v}(r)$ and the number of particles in the ring $M(R,t)$ were measured. Contact line pinning is produced by surface irregularities and is much stronger with the solute than without it. The ring deposit can create surface unevenness as well as augment the surface imperfections that produced the initial pinning.

The depth-averaged velocity $\bar{v}(r)$ for thin drops, with $\theta_c \simeq 0$, shows the predicted $(R-r)^{-.5}$ divergence in the vicinity of the contact line. The measured ring mass $M(R,t)$ is plotted in Figure 3. These drops had an initial contact angle $\theta_c \simeq .25$ radians. For this angle, our theory predicts an initial increase $M(R,t) \sim t^{1.37}$. This behavior is not expected at very early times ($t \lesssim (4R)^2/D \simeq 10$ sec), before steady-state diffusion has been achieved. To account for transient effects during this early period, we allow a shift in the effective starting time of order 10 sec. We also include an offset in the deposited mass in order to account for the particles deposited during the initial transient. Choosing the M and t offsets to achieve the best straight line on a log-log plot yielded power-law fits $M - M_0 \sim (t+t_0)^p$, where $p = 1.3 \pm 0.1$. Thus the expected initial growth of the ring is consistent with observation. To predict the growth of the ring at later times, we first determine $\bar{v}(r)$ numerically from the known flux $J(r)$ of a thick drop and then use this $\bar{v}(r)$ to determine $M(R,t)$ as outlined after Eq. (1) above. This predicted $M(R,t)$ is compared with the data in the inset of Figure 3. Again the prediction is in good agreement with the data.

Several effects modify the simplified theory sketched above. Noncircular drops must have uneven deposition rates: highly convex regions have a stronger evaporating flux and thus denser deposits, as corroborated by Figure 1a. If the solute is not dilute, the ring deposit is forced to have a nonzero width; higher initial concentration leads to a wider ring. Further thermodynamic effects may modify the flow and the ring deposition. Some solutes may segregate to the solid surface and become immobilized. Others may segregate to the free surface where the outward flow is faster than $\bar{v}$. The thermal and concentration gradients caused by evaporation can lead to circulating surface-tension-gradient driven (i.e., Marangoni) flows. These can interfere with the outward flow discussed above. Our experiments showed both surface segregation and circulating flow but their impact was minor (as we will discuss in detail elsewhere). High viscosity in the liquid can also modify the deposition by preventing the drop from attaining an equilibrium droplet shape. We estimate that in our experiments such viscous effects should be negligible except within a few microns of the contact line.

Our measurements support this capillary flow mechanism for contact-line deposition. They show that the deposition can be predicted and controlled without knowing the chemical nature of the liquid, solute or substrate. The model accounts in a natural way for the nearly complete transport of the solute to the periphery. By controlling the speed and spatial variation of the evaporation, this model predicts that we can control the shape and thickness of the deposit. Often it is desired to deposit solute particles in a confined region as in for example the printing of fine lines [5]. The commonplace ring stain appears to provide a simple and robust route to such confinement.

---

[1] Parisse, F. and Allain, C., "Shape Changes of Colloidal Suspension Droplets during Drying" *J. Phys II*, **6** 1111-1119 (1996).

[2] El Bediwi, A. B., Kulnis, W. J., Luo, Y., Woodland, D., and Unertl, W. N., "Distributions of Latex Particles Deposited from Water Suspensions" *Mat. Res. S oc. Symp. Proc.*, **372** 277-282 (1995).

[3] Denkov, N. D., Velev, O. D., Kralchevsky, P. A., Ivanov, I. B., Yoshimura, H., and Nagayama, K. "Mechanism of Formation of Two-Dimensional Crystals from Latex Particles on Substrates" *Langmuir*, **8** 3183-3190 (1992).

[4] Laden, P. ed.*Chemistry and technology of water based inks* (London, Blackie Academic & Professional, 1997)

[5] Society for Imaging Science and Technology, *1996 TAPPI New Printing Technologies Symposium : proceedings* (Atlanta, GA : Tappi press,1996)

[6] Hisatake, K., Tanaka, S. Aizawa, Y., "Evaporation of Water in a Vessel" *J. Appl. Phys.* **73** 7395-7401 (1993).

[7] Peiss, C. N., "Evaporation of Small Water Drops Maintained at Constant Volume" *J. Appl. Phys* **65**5235-5237 (1989).

[8] Maxwell, J. C. *Scientific Papers* vol. 2 (Cambridge, 1890).

[9] Jackson, J. D.*Classical Electrodynamics*, 2nd edition (J. Wiley, New York, 1975) p. 77.

[10] Lide, D. R. ed.*CRC Handbook of Physics and Chemistry* 77th edition, Chemical Rubber Publishing Company (Boca Raton FL, 1996). pp **6**-218 **6**-8.

[11] Crocker, J. C. and Grier, D. G. "Methods of Digital Video Microscopy for Colloidal Studies" *J. Colloid and Interface Science*, **179** 298-310 (1996).

ACKNOWLEDGMENTS: The authors cordially thank Hao Li, Xiangdong Shi and Michelle Baildon for their

early contributions to this project, John Crocker, David Grier, and Andy Marcus for sharing with us their expertise, their image analysis code, and their facilities, and to Steve Garoff, L. Mahadevan, Sergei Esipov, Robert Leheny, Dan Mueth, Ed Ehrichs, Jim Knight, Sean Blanton, Narayanan Menon, Jeff Cina and Leo Kadanoff for stimulating discussions. This work was supported by grants from NSF-MRSEC, NSF, and DOE.

CORRESPONDENCE should be addressed to RDD (rddeegan@control.uchicago.edu). Further information may be found on the internet at http://MRSEC.uchicago.edu/MRSEC